

Research Articles | Behavioral/Cognitive

Long-horizon associative learning explains human sensitivity to statistical and network structures in auditory sequences

<https://doi.org/10.1523/JNEUROSCI.1369-23.2024>

Received: 4 July 2023

Revised: 16 January 2024

Accepted: 7 February 2024

Copyright © 2024 the authors

This Early Release article has been peer reviewed and accepted, but has not been through the composition and copyediting processes. The final version may differ slightly in style or formatting and will contain links to any extended data.

Alerts: Sign up at www.jneurosci.org/alerts to receive customized email alerts when the fully formatted version of this article is published.

1 **Title** Long-horizon associative learning explains human sensitivity to statistical and network structures in auditory
2 sequences

3

4

5 **Abbreviated Title:** Neural encoding of community network structures

6

7

8

9 **Authors:** Lucas Benjamin¹, Mathias Sablé-Meyer^{1,2}, Ana Fló^{1,3}, Ghislaine Dehaene-Lambertz^{1*}, Fosca Al Roumi^{1*}
10 * Contributed equally

11

12

13 **Affiliations:** 1 Cognitive Neuroimaging Unit, CNRS ERL 9003, INSERM U992, CEA, Université Paris-Saclay, NeuroSpin
14 Center, Gif/Yvette, France

15

2 Sainsbury Wellcome Centre for Neural Circuits and Behaviour, University College London, London, UK

16

3 Department of Developmental Psychology and Socialization, University of Padova, Padova, Italy

17

18

19

20

21 **Corresponding author:** Lucas Benjamin: lucas.benjamin78@gmail.com

22

23 **Number of pages:** 15

24

25 **Number of figures:** 4

26

27 **Number of words for abstract:** 225

28 **Number of words for significance statement:** 95

29 **Number of words for introduction:** 648

30 **Number of words for discussion:** 1455

31

32 **Conflict of interest statement:** The authors declare no conflict of interest

33

34 **Acknowledgments:**

35 We thank Lucia Melloni for discussions and remarks during the data analysis.

36

37

38

JNeurosci Accepted Manuscript

41 Abstract

42

43 Networks are a useful mathematical tool for capturing the complexity of the world. In a previous behavioral study, we
44 showed that human adults (N=23, 16 females) were sensitive to the high-level network structure underlying auditory
45 sequences, even when presented with incomplete information. Their performance was best explained by a
46 mathematical model compatible with associative learning principles, based on the integration of the transition
47 probabilities between adjacent and non-adjacent elements with a memory decay. In the present study, we explored
48 the neural correlates of this hypothesis via magnetoencephalography (MEG). Participants passively listened to
49 sequences of tones organized in a sparse community network structure comprising two communities. An early
50 difference (~150 ms) was observed in the brain responses to tone transitions with similar transition probability but
51 occurring either within or between communities. This result implies a rapid and automatic encoding of the sequence
52 structure. Using time-resolved decoding, we estimated the duration and overlap of the representation of each tone.
53 The decoding performance exhibited exponential decay, resulting in a significant overlap between the representations
54 of successive tones. Based on this extended decay profile, we estimated a long-horizon associative learning novelty
55 index for each transition and found a correlation of this measure with the MEG signal. Overall, our study sheds light on
56 the neural mechanisms underlying human sensitivity to network structures and highlights the potential role of
57 Hebbian-like mechanisms in supporting learning at various temporal scales.

58

59

60

61 Significance statement

62

63 We conducted a MEG study in which human adults were passively exposed to sequences of tones organized in a
64 sparse community network structure. Despite the uniform transition probabilities between tones, participants' brain
65 activity exhibited sensitivity to the network structure. Notably, a consistent “deviant” response was observed at ~150
66 ms when the sequence switched between communities. A long-tail exponential decay in tone representation allowed
67 overlapping representations of successive sequence elements, facilitating long-range associative mechanisms. This
68 binding mechanism adequately accounted for various scales of sequence learning, bridging the gap between statistical
69 and network learning approaches.

70

71 Introduction

72 Understanding the structure of the input sequences we encounter is fundamental for developing a comprehensive
73 mental model of our environment (*Dehaene et al., 2022, 2015*). The capacity to detect first-order relationships between
74 successive events (i.e., transition probabilities) and its limits have been extensively studied in humans at the behavioral
75 and neural levels (*Benjamin et al., 2021, 2023b, 2024; Fló et al., 2022; Henin et al., 2021; Maheu et al., 2019; Saffran et al.,*
76 *1996*) as well as in non-humans animals (*Boros et al., 2021; James et al., 2020; Toro and Trobalón, 2005*). Higher-order
77 statistical relations between elements of a sequence are also detected by human adults and children (*Karuza et al.,*
78 *2019, 2019; Lynn et al., 2020; Mark et al., 2020; Schapiro et al., 2013*), but only a limited number of neuroimaging studies
79 have explored possible neural correlates of this learning (*Ren et al., 2022; Schapiro et al., 2016; Stiso et al., 2022*).
80 Therefore, we still do not know if a single mechanism can adequately explain both first order (local transitions) and
81 network structure learning or if these computations require distinct cognitive and brain processes.

82 To bridge the gap between local statistical and network-level learning studies, we previously proposed the *sparse*
83 *community paradigm*, which allows to simultaneously characterize these aspects on auditory sequences (*Benjamin et*
84 *al., 2023a*). Building upon the community paradigm introduced by *Schapiro et al (2013)*, we created a network consisting
85 of two densely but incompletely connected clusters (called communities) of six elements each. Each element is
86 connected with four other elements, and the two clusters are linked by only two edges (links). A learning sequence is
87 created by randomly drawing the next tone from the four possibilities, creating a random walk in the network with a
88 uniform transition probability (TP) between successive tones (Movie 1A). After exposure to such a sequence,
89 participants were asked to judge their familiarity with various pairs of tones that 1) had or had not been presented
90 during learning to test local TP learning, and 2) did or did not belong to the same community to test learning of the
91 higher-level structure (*Benjamin et al., 2023a*). Interestingly, participants judged new transitions they had never heard
92 as highly familiar if they were between tones belonging to the same community. This *completion* effect demonstrated
93 that they generalized the community structure to missing transitions. Conversely, they judged transitions between
94 communities to be less familiar than within communities despite the absence of any difference in local transition
95 probability during learning. This *pruning* effect translates into a decrease in subjective familiarity with tone pairs that
96 switch from one community to the other despite similar transition probabilities between tones. Among the various
97 models proposed in the statistical and network learning literature, an associative learning approach (the free energy
98 minimization model - FEMM (*Lynn et al., 2020*)), conceptually related to the successor representation, provided the
99 best fit to participants' behavior. According to this model, participants did not solely compute adjacent transition
100 probabilities but a linear sum of transition probabilities at all orders (adjacent, first-order non-adjacent, second-order
101 non-adjacent and so on), weighted by a decreasing exponential factor. This model explains how both local transitions
102 and network structures are perceived, and successfully accounts for behavioral results across different network types,
103 including community, sparse community, ring, and lattice networks (*Benjamin et al., 2023a; Lynn et al., 2020*), as well as
104 results concerning local statistical learning. FEMM appears to be a good candidate for a unifying framework of
105 sequence learning.

106
107 However, a common model is insufficient to postulate a common implementation (*Marr, 1982*) and there is still no
108 consensus on how the brain implements these computations. On the one hand, sensitivity to network structure is
109 often described as a conscious abstraction of the structure involving top-down attention processes with late brain
110 signatures (*Ren et al., 2022*) typically in the prefrontal cortex (*Stiso et al., 2022*). On the other hand, we previously
111 postulated that low-level associative learning (*Benjamin et al., 2023a; see also Endress, 2010; Endress and Johnson, 2021;*
112 *Schapiro et al., 2017*) was sufficient for both local and higher-order learning. To disentangle those two hypotheses, we
113 tested here whether passive exposure to a rapid auditory sequence could lead to successful learning of its network
114 structure. We thus exposed participants to fast sequence of tones following the sparse community design while
115 recording their brain activity with MEG.

116

117 Materials and methods

118 Stimuli and procedure

119 We generated twelve tones of 50ms duration, logarithmically distributed from 300 to 1800 Hz. For each participant,
120 the twelve tones were randomly assigned to the twelve nodes of the sparse community network (see Movie 1 for a
121 complete description of the network structure). The sparse community network comprised two communities (i.e.,
122 clusters) made of six nodes, densely connected to each other but poorly connected to the nodes of the other
123 community. Crucially, in the *sparse* community design, some connections between nodes belonging to the same
124 community are missing. Specifically, for each participant, we randomly removed twelve transitions (6 per community,
125 one per node). After a training block with this incomplete graph, new transitions were added at a low frequency (4%)
126 for the following test blocks. We refer to these transitions as *New* and those presented during training as *Familiar*. The
127 *New* transitions were critically within and between the communities (which we refer to as *Within vs Between*). *New*
128 *Within* corresponds to the twelve 'missing' transitions randomly removed from the network in the training block. To
129 balance, we randomly selected 12 *New Between* transitions (one per node) that violated the community clustering
130 property. As a result, the transition probabilities between tones during the training block were flat: TP = 25%, while
131 during the test blocks, the *Familiar* transitions had TP = 23% and a frequency of 18.4/block. The 12 *New Within* and 12
132 *New Between* community transitions had TP = 4% and a frequency of 3.2/block. The *New Within* and *New Between*
133 transitions were randomly drawn for each subject to add variability to the network structure. Movie 1A shows an
134 example of one structure and the associated sequence used for one participant.

135 We then performed random walks in the participant's sparse community graph to derive one 960 items-long training
136 sequence and six 960 items-long test sequences (one sequence corresponds to one block) with 200ms inter stimulus
137 interval (ISI) between each tone (Movie 1A). The first block of 960 items comprised only *Familiar Within* and *Familiar*
138 *Between* transitions (training block, TP = 25% each). For the next six blocks (Test 1-6), we introduced infrequent *New*
139 *Within* and *New Between* transitions (TP = 4% each). All *Familiar* transitions, independently of whether they were
140 *Within* or *Between* communities, had the same TPs and appeared with the same frequency (TP = 23% each). However,
141 the graph structure entails that the participants heard in total fewer between community transitions than within
142 community transitions (there are 32 *Familiar Within* and 4 *Familiar Between* community transitions during training,
143 completed by 12 *New Within* and 12 *New Between* community transitions during test).

144

145 Crucially, the experiment was completely passive, and participants were unaware of the structure of the auditory
146 sequence. They were only instructed to pay attention to the sequence of tones and to stay still while looking at a
147 fixation cross displayed at the center of the screen to avoid noise from eye movements. The experiment lasted around
148 45 minutes, and a small break inside the MEG was possible between each block.

149

150

151 Participants

152 29 healthy adults came to the lab and 23 recordings (16 females, mean age = 26.58, sd = 6.1) were kept for the
153 analyses (4 subjects were rejected due to MEG malfunction, 1 due to experimenter error during recording, and 1 scan
154 was aborted due to subject agitation). All participants gave written informed consent prior to enrollment and received
155 90€ as compensation. This experiment was approved by the national ethical committee (CPP Ile-de-France III).

156

157 MEG recordings and preprocessing

158 Participants performed the tasks while sitting inside an electromagnetically shielded room. The magnetic component
159 of their brain activity was recorded with a 306-channel, whole-head MEG by Elekta Neuromag® (Helsinki, Finland). The
160 MEG helmet is composed of 102 triplets, each comprising one magnetometer and two orthogonal planar
161 gradiometers. Brain signal was acquired at a sampling rate of 1000 Hz with a hardware high-pass filter at 0.03Hz. The
162 data were then resampled at 250Hz to reduce computational load. Eye movements were monitored with vertical and
163 horizontal EOGs and heartbeats with ECGs. Subjects' head position inside the helmet was measured for realignment at
164 the beginning of each run with an isotrack Polhemus Inc. system from the location of four coils placed over the frontal
165 and mastoids.

166 MEG signal was then preprocessed using MNE python pipeline with classical steps following recommendations from
167 (*Jas et al., 2018; Niso et al., 2018*). We first applied Maxfilter algorithm to remove ambient noise, and signal was band-
168 pass filtered ([0.1-30] Hz). Eye movements and heartbeats were identified and removed using PCA components'
169 correlation with EOG and ECG measures.

170 To decode if a transition was within or between community, data was epoched from 100 ms before to 300ms after
171 tone onset. To determine how sustained was the neural representation of each tone across time, we segmented the
172 data in 2.6 seconds long epochs, from 100 ms before to 2500 ms after tone onset. Bad data, channels, and epochs
173 were detected and removed with autoreject toolbox (*Jas et al., 2017*).

174

175 Within vs Between Decoding analysis

176 To examine whether the brain encoded the community structure, we trained a logistic regression decoder to predict
177 whether the transition that just occurred stayed *Within* a community (*Familiar Within* and *New Within*) or switched
178 *Between* communities (*Familiar Between* and *New Between*). The decoder was trained on the short epochs ([-0.1, 0.3])
179 slightly smoothed using a sliding window (± 20 ms) to enhance the signal-to-noise ratio. We used 3 folds cross-
180 validation process: the decoder was trained on 2/3 of the data and tested on the remaining third of the trials. The
181 procedure was repeated three times, corresponding to the 3 cross-validation folds. Each transition had the same
182 frequency but *Within* transitions were more numerous than *Between* transitions, resulting in a larger total number of
183 epochs for *Within* condition. We thus used the area under the ROC curve as a metric of success (ROC AUC) since it is
184 not sensitive to such imbalance. This analysis was conducted for each time-point of the epochs (fig 1). We also
185 computed the decoding performance when the decoder was trained at time t and tested at time t' , to reveal the
186 generalization across time (GAT) of the decoder, and thus the stability of the mental representation (fig 1). By design,
187 the diagonal of the GAT matrix corresponds to the previously described time-by-time decoding performance.

188 To assess robustness, we replicated the decoding accuracy with a different metric, we performed a decoding analysis
189 on the whole epoch at the subject level for training and testing. This decoder simultaneously used all time points
190 across all recording channels, providing a single accuracy value for the entire epoch. Unlike time-by-time decoding, this
191 approach can exploit the temporal dynamic of the signal to differentiate conditions.

192 For the previous analysis, we pulled together the data from *Familiar* and *New* transitions. In a further analysis, we
193 investigated whether the success of decoding the community remained possible when analyzing *Familiar* and *New*
194 transitions separately. Therefore, we replicated the previous decoding analysis but limited it to *Familiar* transitions
195 only, which had identical high local transition probabilities of 23% (*Familiar Within Vs Familiar Between*), or to *New*
196 transitions only (*New Within Vs New Between*), which had a low transition probability of 4%. Note, however, that in
197 this last case, the number of epochs was small, resulting in a low signal to noise ratio.

198

200 Statistical significance in the Generalization Across Time (GAT) matrix was assessed using a temporal-temporal cluster-
201 based permutation (MNE python (*Gramfort et al., 2013*)) for times between 0 and 300ms. For the time-by-time decoder,
202 we performed a temporal cluster permutation test in [0, 300]ms time window. Note that these two statistical tests are
203 not independent as the time-by-time decoding corresponds to the diagonal of the GAT Matrix. The whole epoch
204 decoding gives a single decoding value per subject, we thus performed a one-way t-test across subjects to test
205 whether the decoding performance was significantly above-chance.

206

207 Long-horizon associative learning estimation and linear regression

208 To assess the duration of the representation of a sequence item in the brain signals, we used epochs containing 10
209 tones (2.5s). We trained a 12-class decoder (for the 12 tones) with balanced accuracy to decode the identity of the first
210 tone of the epoch throughout the whole epoch. To ensure that we were decoding the sustained activity related to the
211 first tone and not a subsequent repetition of the same tone, we removed from the analysis all epochs in which the first
212 tone was repeated during the test window ($\sim 65\%$ of the epochs were removed, fig 3A). We averaged the above
213 chance decoding performance over the time-windows (250ms), which corresponded to the interval between two
214 consecutive items, to estimate the amount of superposition of the representations of the different elements of the
215 sequence. We then estimated the long-horizon associative learning strength of the association for each pair (\hat{A}), which
216 corresponds to the sum of the transition probability matrix between the tones at all orders (A^t), weighted by the
217 overlap between item representations (fig 3B).

218 We later used the associated novelty index, defined as the negative log of this association strength, as a regressor for
219 the MEG signal during the short epochs corresponding to the different transition types (fig 3D). We performed spatio-
220 temporal cluster analysis on the beta value associated with this linear regression to extract electrodes and times
221 where this long-horizon associative learning estimation might significantly explain the difference in activity across
222 conditions. We also computed the average association strength of each type of transition (fig 3C).

223

224 Results

225

226 Our experiment aimed to identify the neural correlates of community structure encoding and evaluate if this learning
227 stems from a low-level associative process or corresponds to a late and explicit discovery (*Ren et al., 2022; Stiso et al.,*
228 *2022*). To assess the encoding of the community structure, we first decoded *Within* vs *Between* transition type to
229 characterize the temporal dynamics of the representation of each tone in the sequence in order to assess the
230 possibility of overlapping representations that might allow long-distance associations. Based on this measured overlap,
231 we could estimate the long-horizon associative familiarity for each transition. Finally, to determine whether this long-
232 horizon associative learning model was indeed a plausible hypothesis, we ran a linear regression between the
233 predicted familiarity and our data.

234

235 Decoding Within Vs Between community transitions

236 We first tested whether participants' mental model of the sequence encoded the community structure despite
237 uniform transition probabilities. We thus trained and tested decoders on all tone epochs ending in a *Within* transition
238 vs all tone epochs ending in a *Between* transition on all pairs (*Familiar* and *New*). We obtained a significant cluster

239 (p<0.05) in the GAT matrix accuracy. Temporal cluster analysis on the Time-by-Time decoding accuracy revealed a
240 significant cluster between 90 and 250ms (p<0.001), peaking at 160ms. Finally, the epoch-based decoding was
241 significantly above chance (p<0.01) (see fig 1 *Within vs. Between*).

242 We then restricted this analysis to the *Familiar* transitions (*Familiar Within vs. Familiar Between*, which corresponds to
243 92% of the epochs). Since *Familiar Within* and *Familiar Between* transitions have the same transition probabilities
244 (0.23), a significant difference would then be due to a higher-order representation of the community structure. Here
245 again, a significant cluster (p<0.01) was found in the GAT matrix. A temporal cluster between 80 and 280ms was found
246 in the time-by-time decoding (p<0.001) with a peak at 150ms. Epoch-based decoding was also significantly above
247 chance (p<0.001).

248 Symmetrically, we restricted the analysis to *New* transitions only (*New Within vs. New Between*, which corresponds to
249 8% of the epochs). By design, both *New Within* and *New Between* transitions had transition probabilities of 4% so
250 learning only local transition probabilities would predict equal unfamiliarity with both types of transition. In line with
251 the previous results, we found a significant temporal-temporal cluster in the generalization matrix (p<0.05), and a
252 significant temporal cluster in the time-by-time decoding (p<0.05, significant time = [130, 170] ms, peaking at 160ms).
253 Epoch based decoding was also significant (p<0.05). Due to the much smaller number of epochs, the results were
254 noisier.

255 We also computed the ERF on the gradiometers for the *Familiar Within vs Familiar Between* and *New Within vs New*
256 *Between* contrasts on the [100-200]ms time-window to confirm the presence of the effect found with the decoding
257 approach. The outcomes were qualitatively comparable: a significant effect around 150 ms for the *Familiar Within vs.*
258 *Familiar Between* contrast (cluster-based permutations p<0.001), and a trend effect for the *New Within vs. New*
259 *Between* contrast (cluster-based permutations p=0.075). In both cases, the topography of the difference was
260 compatible with an auditory response.

261

262 We performed a series of control analyses to eliminate putative low-level confounds, such as decoding success based
263 on the identity of the current tone, the previous tone, or the pair of tones. To control for tone identity decoding, we
264 ran the decoding analysis but restricted it to one of the four nodes at the border of a community (i.e., connected to a
265 node of the other community, darker nodes in fig 2). Depending on the previous tone, these epochs could be either
266 *Familiar Within*, *Familiar Between*, *New Within*, or *New Between*. Thus, decoding within vs between community
267 transitions on those epochs cannot be driven by the tone identity. The same was done for epochs where the transition
268 began with one of these four nodes (i.e., epochs where the previous node of the sequence was one of the nodes at the
269 border of communities) to control for decoding the identity of the previous tone. We also controlled for the pair
270 forming the transition (previous and current tone identity simultaneously): in a similar manner to the current tone
271 control, we restricted the analysis to nodes at the borders of communities and also cross-validated the decoding on
272 the previous tone identity. To do so, we trained and tested our decoder on different previous nodes (training on three
273 previous nodes per community and testing on the three others, see batches in fig 2). This strategy was also used for
274 the *Familiar Within Vs Familiar Between* Generalization Across Time matrix (GAT) decoder. By experimental design,
275 *New Within vs. New Between* decoders were already balanced for current and previous tones (each node is attached
276 to one transition of each type). Thus, we only controlled for the pair by using the cross-validation of the previous node
277 with the same batches described above. Overall, the control analyses qualitatively and quantitatively confirmed
278 previous results. Only the *New Within vs. New Between* control for pair (i.e. controlling both previous and current tone
279 identity simultaneously) analysis did not reach significance, probably due to the small number of epochs in this
280 analysis (only 8% of the data was used in this last control).

281

282 *Within vs Between* community transitions decoding could also rely on a habituation effect. Indeed, if the sequence
283 remains within a community, a particular sound might be repeated multiple times within a short span, causing
284 habituation. However, if the sequence shifts from one community to another, the same sound is less likely to be
285 repeated in a short time, thus preventing habituation. Therefore, this differential habituation effect could drive the
286 *Within vs. Between* decoder. To rule out this alternative hypothesis, we restricted the analysis to the first appearance
287 of each tone after a community change. Thus, close repetitions of tones of the same community are avoided in the
288 data used for this decoder. Despite a decrease in the number of epochs, the decoding accuracy of those controls was
289 still significant for all conditions. All generalization matrices are shown in fig 2.

290

291 Long-horizon associative learning estimation

292 We tested here the hypothesis that long-horizon associative learning (associative learning over several consecutive
293 and non-consecutive items) can support the encoding of network structure. This concept builds on Hebb's principle of
294 strengthening the link between co-occurring events. Nonetheless, instead of focusing solely on learning adjacent pairs,
295 we proposed a broader approach that allows connections to be established over longer distances. In our experiment,
296 this long-horizon associative learning implies that the mental representation of each tone is sustained for a sufficient
297 duration to allow several tones to overlap (*Endress, 2010*) and thus enable associations through more successive tones.
298 According to this model, it is predicted that the representation of each tone should decrease following an exponential
299 profile. To test this hypothesis, we quantified the overlap between the representations of item n and item $n+i$. In fact,
300 this provides a good estimator of the weight of the non-adjacent transition probability of order i .

301 To estimate the overlap between brain representations of different items of the sequence, we determined how long
302 the representation of each item was seen in brain activity. To do so, we split the data into 10-items long sequences
303 (i.e. 2.5 seconds) with no repetition of the first tone in the sequence. We train a 12-class decoder on each time-point
304 to predict the identity of the first tone. Decoding performance is shown in fig 3. We averaged the above chance
305 decoding performance over the time-windows corresponding to the interval between two consecutive items. We
306 observed an exponential-like decrease in performance that reached 0 after ~ 8 sequence items (fig 3A). It shows that
307 the overlap enabling associative learning might thus include long-horizon dependencies of up to 8 items.

308 We estimated the long-horizon associative learning strength of each pair of tones. To do so, we computed the sum of
309 the different transitional probability orders weighted by the overlap between item representations as estimated from
310 the decoding performances (fig 3B). This gave us a 12x12 symmetrical matrix of learning familiarity for each pair (fig
311 3C). Finally, we averaged this measure of Familiarity for each condition type (fig 3C) and obtained a result that is
312 consistent with the pruning effect (difference between *Familiar Within vs Familiar Between* transitions) and the
313 completion effect (difference between *New Within* and *New Between* transitions) as discussed in (*Benjamin et al.,*
314 *2023a*).

315

316

317 Long-horizon associative learning accounts for epoch variability

318 To test the neural predictions of long-horizon associative learning, we correlated brain signals with the estimated
319 associative learning strength of each transition (fig 3D). We performed a linear regression between the brain signal
320 after each tone and the novelty effect produced by each transition. Unlike most studies of sequence learning, where
321 the novelty is calculated solely from local transition probabilities, we computed it here as the negative log of the long-
322 horizon associative learning strength. This calculation takes into account several orders of adjacent and non-adjacent
323 transition probabilities whose weights have been computed based on the overlap of brain representations estimated
324 by our tone decoder (fig 3 A-D). A spatio-temporal cluster permutation test revealed a significant cluster (fig 3E) in the

325 magnetometers (right centro-occipital, time = [150 ; 290] ms, $p_{val} < 0.01$) that was replicated in the gradiometers
326 (right centro-occipital, time = [140 ; 300] ms, $p_{val} < 0.05$).

327 Furthermore, the observed clusters were still significant when the negative log of the adjacent transition probabilities
328 was introduced as a supplementary regressor ($p_s < 0.05$ for both magnetometers and gradiometers clusters).
329 However, if the high correlation between the TP matrix and the long horizon-associative model makes it hard to
330 directly disentangle those two models solely based on this regression analysis, it does nicely complement the decoding
331 analyses.

332

333

334 Discussion

335

336 In this study, our aim was to determine whether local statistical learning and structure learning in sequences are
337 governed by the same cognitive process or by distinct processes. Learning local statistics is often described as an
338 associative process, while network learning is usually seen as an abstract map representation. Previous studies
339 exploring network learning have used explicit paradigms, revealing late brain signatures consistent with top-down or
340 frontal activity (*Ren et al., 2022; Stiso et al., 2022*). However, based on a modeling approach, we proposed in our
341 previous behavioral study that low-level associative learning strategies might support both local and high-order
342 statistical scales (*Benjamin et al., 2023a*). Thus, this hypothesis predicts that learning sequence structure does not
343 require an explicit representation and may instead rely on automatic and rapid (~150ms) mismatch responses, similar
344 to those observed after the violation of local transition probabilities.

345

346 Network learning results from a low-level bottom-up computations

347 To test these predictions, we presented participants with a passive learning task using rapid auditory sequences. We
348 showed that the structure properties of the sequence were rapidly decodable from the participants' brain recordings
349 (~[100-250] ms after tone onset). The timing of this response, as early as 150ms after the information became
350 available, aligns with the rapid deviant responses (MMN in EEG) observed in learning based on violation of transitional
351 probabilities (*Maheu et al., 2019; Todorovic and de Lange, 2012*). Since the transition probabilities between tones were
352 uniform and the walk within the network was random, prediction could not be based on high-level top-down
353 expectation. This early and automatic response (150 ms after the transition) challenges the notion of abstract and
354 explicit calculations as prerequisites for learning such structures. In addition, our analyses revealed a similar effect
355 when the decoding analysis was restricted to new transitions (*New Within Vs New Between*) and to familiar transitions
356 (*Familiar Within Vs Familiar Between*), suggesting an automatic generalization of the community structure beyond
357 sensory evidence. This result provides a neural underpinning for the behavioral observations we previously reported,
358 indicating that participants accurately assess the familiarity of transitions based on their congruence with network
359 structure, even when these transitions were not encountered during training.

360

361 Long-horizon associative learning as a plausible implementation for FEMM

362 In our previous study, we hypothesized that the FEMM could effectively explain adult behavioral performance. This
363 model aggregates the different orders of statistical regularities (adjacent and non-adjacent) into a single quantity. In
364 this study, we showed that this model can be readily implemented through a simple associative learning mechanism

365 relying on Hebb's principle (*Benjamin et al., 2023a; Hebb, 1949*). In the context of structure learning, this principle would
366 imply a sustained mental representation of each tone for a sufficient duration to enable the overlapping of several
367 elements despite the temporal distance. We thus predicted the representation of each tone to exhibit an exponential
368 decay profile. A rapid decay of tone information would limit associations to short distances, while a slower decay
369 would facilitate the formation of long-horizon dependencies and, therefore, the extraction of the underlying structure.
370 Thus, this exponential decay acts as a balance between local relevance and generalization.

371 To test this idea, we estimated the duration of the representation of each tone, performing a decoding analysis of tone
372 identity. The identity of a tone was decodable during the presentation of the subsequent eight tones, with a decoding
373 performance exponentially decaying over subsequent tones. This profile provided an estimation of the number of
374 elements simultaneously represented at a given time. Consequently, it allowed us to quantitatively assess the strength
375 of each tone pair in the heard sequence (fig 3C). We found that these weights accurately accounted for the results of
376 the *Within vs. Between* decoders, encompassing both *Familiar* and *New* transitions (Fig. 4D). Moreover, this estimated
377 strength significantly correlated with neural activity, aligning with the timing of the automatic deviant response
378 (*Maheu et al., 2019; Todorovic and de Lange, 2012*). This result provides compelling evidence for the rapid encoding of
379 structure through bottom-up processes compatible with associative learning strategies.

380 However, it is worth noting that an alternative implementation of the same metric is theoretically possible. Simple
381 pairwise association learning, in combination with a transitivity property, would also predict similar learning. In fact, if
382 participants solely learn pairs (e.g., A-C and C-D), transitivity of this learning can strengthen the A-D pair, even if not
383 explicitly presented. Considering this transitivity with similar exponentially decreasing weights would be
384 mathematically equivalent to our model while not strictly requiring a sequential presentation of the structure.
385 Although, we cannot definitively rule out this alternative implementation of the same metric, our findings suggest that
386 sequential presentation is crucial to have an overlap between successive items representations, enabling Hebbian
387 associative learning. It is also important to acknowledge that associative learning might not be the sole mechanism
388 contributing to network structure learning, particularly in cases where explicit detection is required from participants.
389 Abstract representations of hippocampal maps (*Constantinescu et al., 2016*) or frontal maps (*Stiso et al., 2022*) might also
390 play a role in such tasks (*Garvert et al., 2017; Schapiro et al., 2017, 2016*). Intracranial recordings conducted during local
391 statistical learning paradigms have revealed that multiple brain regions, including cortical areas and hippocampus, can
392 simultaneously represent the same structure while carrying different information (*Henin et al., 2021*).

393

394

395 [Difference between implicit passive listening and explicit structure learning](#)

396 Thus, converging results provide evidence that associative learning supports the perception of the community
397 structure in the present experiment. Long-horizon associative learning strength significantly accounted for the
398 variance in brain signals (fig 3E). Moreover, the pruning and completion effects found with decoders (fig 1) can easily
399 be explained by the same mechanism (see fig 3D). However, it is worth noting that the results from our previous
400 behavioral study do not entirely align with the current ones. Specifically, in the present experiment, the representation
401 of tones exhibited a more rapid decrease (exponential decrease factor 0.52) as compared to its estimation in our
402 previous behavioral study (factor 0.058, about ten times lower). This discrepancy suggests that participants in the
403 current experiment might be less inclined to generalize the underlying structure.

404 Several factors might explain this difference. Firstly, the generalization factor estimation in the MEG experiment may
405 be noisier due to the small number of participants (23 vs. several hundred in the behavioral study). Since the trade-off
406 between generalization and accuracy may vary among individuals (*Lynn et al., 2020*), on one side group level estimation
407 with 23 subjects is limited and on the other side at the individual level, it is difficult to measure this trade-off due to
408 the data variability. A larger sample size with multiple sessions per subject would be necessary to obtain a reliable

409 estimation of the generalization factor at the individual level. Secondly, it is possible that associative learning
410 represents the implicit component of this task (*Andringa and Rebuschat, 2015*), followed subsequently by an explicit
411 decision-making process involving higher level prefrontal regions. This second step might facilitate the abstraction of
412 the structure by labeling each community as distinct (*Koechlin et al., 2003; Koechlin and Jubault, 2006*). This dual process
413 could explain why explicit behavioral tasks (*Benjamin et al., 2023a; Lynn et al., 2020*) exhibit a better generalization
414 factor compared to our implicit MEG task. The same explanation may account for the late signatures of top-down
415 activity reported by (*Ren et al., 2022*) who used a slow and explicit task. To further explore this hypothesis, a direct
416 comparison of passive and active learning of such networks while monitoring the representations in the auditory
417 cortex, the hippocampus, and the lateral prefrontal cortex would be necessary.

418

419

420 Conclusion

421 The aim of the present study was to uncover the neural mechanism underlying network learning. We proposed the
422 sparse community paradigm as a way of combining local statistical learning and network learning in a single sequence.
423 Previous behavioral studies have shown that a mathematical model (FEMM) accurately captures human learning.
424 Here, we add that the behavioral pattern described by the FEMM is compatible with certain associative learning
425 principles. Indeed, thanks to time-by-time decoding of the brain state associated with a tone, we observed an
426 exponential decay in the tone representation across 8 elements. Using this estimate of mental representations'
427 dynamics, we estimated the strength of each network transition. This estimate significantly correlated with our data.
428 The present study provides novel insights into the mechanism underlying network learning and highlights the
429 importance of brain dynamics in the understanding of sequence learning. Further investigations in different
430 experimental conditions (explicit vs implicit), over different tone and ISI durations, with different populations (non-
431 human primates), and during early development are necessary to better characterize this learning ability.

432

433

434

435

436

437

438 Bibliography

- 439 Andringa S, Rebuschat P. 2015. NEW DIRECTIONS IN THE STUDY OF IMPLICIT AND EXPLICIT LEARNING: An Introduction.
440 *Stud Second Lang Acquis* **37**:185–196. doi:10.1017/S027226311500008X
- 441 Benjamin L, Dehaene-Lambertz G, Fló A. 2021. Remarks on the analysis of steady-state responses: spurious artifacts
442 introduced by overlapping epochs. *Cortex*. doi:10.1016/j.cortex.2021.05.023
- 443 Benjamin L, Fló A, Al Roumi F, Dehaene-Lambertz G. 2023a. Humans parsimoniously represent auditory sequences by
444 pruning and completing the underlying network structure. *eLife* **12**:e86430. doi:10.7554/eLife.86430
- 445 Benjamin L, Fló A, Palu M, Naik S, Melloni L, Dehaene-Lambertz G. 2023b. Tracking transitional probabilities and
446 segmenting auditory sequences are dissociable processes in adults and neonates. *Developmental Science* **26**:e13300.
447 doi:10.1111/desc.13300
- 448 Benjamin L, Zang D, Flo A, Qi Z, Su P, Zhou W, Wang L, Wu X, Gui P, Dehaene-Lambertz G. 2024. The role of conscious
449 attention in statistical learning: evidence from patients with impaired consciousness. doi:10.1101/2024.01.08.574591
- 450 Boros M, Magyari L, Török D, Bozsik A, Deme A, Andics A. 2021. Neural processes underlying statistical learning for
451 speech segmentation in dogs. *Current Biology* **31**:5512–5521.e5. doi:10.1016/j.cub.2021.10.017
- 452 Constantinescu AO, Jill O, Behrens TEJ. 2016. Organizing conceptual knowledge in humans with a gridlike code **352**.
- 453 Dehaene S, Al Roumi F, Lakretz Y, Planton S, Sablé-Meyer M. 2022. Symbols and mental programs: a hypothesis about
454 human singularity. *Trends in Cognitive Sciences* **26**:751–766. doi:10.1016/j.tics.2022.06.010
- 455 Dehaene S, Meyniel F, Wacongne C, Wang L, Pallier C. 2015. The Neural Representation of Sequences: From Transition
456 Probabilities to Algebraic Patterns and Linguistic Trees. *Neuron* **88**:2–19. doi:10.1016/j.neuron.2015.09.019
- 457 Endress AD. 2010. Learning melodies from non-adjacent tones. *Acta Psychologica* **135**:182–190.
458 doi:10.1016/j.actpsy.2010.06.005
- 459 Endress AD, Johnson SP. 2021. When forgetting fosters learning: A neural network model for statistical learning.
460 *Cognition* 104621. doi:10.1016/j.cognition.2021.104621
- 461 Fló A, Benjamin L, Palu M, Dehaene-Lambertz G. 2022. Sleeping neonates track transitional probabilities in speech but
462 only retain the first syllable of words. *Scientific Reports* **12**:4391. doi:10.1038/s41598-022-08411-w
- 463 Garvert MM, Dolan RJ, Behrens TEJ. 2017. A map of abstract relational knowledge in the human hippocampal–
464 entorhinal cortex. *eLife* **6**:1–20. doi:10.7554/eLife.17086
- 465 Gramfort A, Luessi M, Larson E, Engemann D, Strohmeier D, Brodbeck C, Goj R, Jas M, Brooks T, Parkkonen L,
466 Hämäläinen M. 2013. MEG and EEG data analysis with MNE-Python. *Frontiers in Neuroscience* **7**.
- 467 Hebb DO. 1949. The organization of behavior: a neuropsychological theory. Mahwah, N.J.: L. Erlbaum Associates.
- 468 Henin S, Turk-Browne NB, Friedman D, Liu A, Dugan P, Flinker A, Doyle W, Devinsky O, Melloni L. 2021. Learning
469 hierarchical sequence representations across human cortex and hippocampus. *Science Advances* **7**:1–13.
470 doi:10.1126/sciadv.abc4530
- 471 James LS, Sun H, Wada K, Sakata JT. 2020. Statistical learning for vocal sequence acquisition in a songbird. *Scientific*
472 *Reports* **10**:1–18. doi:10.1038/s41598-020-58983-8
- 473 Jas M, Engemann DA, Bekhti Y, Raimondo F, Gramfort A. 2017. Autoreject: Automated artifact rejection for MEG and
474 EEG data. *NeuroImage* **159**:417–429. doi:10.1016/j.neuroimage.2017.06.030

- 475 Jas M, Larson E, Engemann DA, Leppäkangas J, Taulu S, Hämäläinen M, Gramfort A. 2018. A Reproducible MEG/EEG
476 Group Study With the MNE Software: Recommendations, Quality Assessments, and Good Practices. *Front Neurosci*
477 **12**:530. doi:10.3389/fnins.2018.00530
- 478 Karuza EA, Kahn AE, Bassett DS. 2019. Human sensitivity to community structure is robust to topological variation.
479 *Complexity* **2019**. doi:10.1155/2019/8379321
- 480 Koechlin E, Jubault T. 2006. Broca's Area and the Hierarchical Organization of Human Behavior. *Neuron* **50**:963–974.
481 doi:10.1016/j.neuron.2006.05.017
- 482 Koechlin E, Ody C, Kouneiher F. 2003. The Architecture of Cognitive Control in the Human Prefrontal Cortex. *Science*
483 **302**:1181–1185. doi:10.1126/science.1088545
- 484 Lynn CW, Kahn AE, Nyema N, Bassett DS. 2020. Abstract representations of events arise from mental errors in learning
485 and memory. *Nature Communications* **11**. doi:10.1038/s41467-020-15146-7
- 486 Maheu M, Dehaene S, Meyniel F. 2019. Brain signatures of a multiscale process of sequence learning in humans. *eLife*
487 **8**:1–24. doi:10.7554/eLife.41541
- 488 Mark S, Moran R, Parr T, Kennerley SW, Behrens TEJ. 2020. Transferring structural knowledge across cognitive maps in
489 humans and models. *Nature Communications* **11**:1–12. doi:10.1038/s41467-020-18254-6
- 490 Marr D. 1982. Vision: a computational investigation into the human representation and processing of visual
491 information. Cambridge, Mass: MIT Press.
- 492 Niso G, Gorgolewski KJ, Bock E, Brooks TL, Flandin G, Gramfort A, Henson RN, Jas M, Litvak V, T. Moreau J, Oostenveld
493 R, Schoffelen J-M, Tadel F, Wexler J, Baillet S. 2018. MEG-BIDS, the brain imaging data structure extended to
494 magnetoencephalography. *Sci Data* **5**:180110. doi:10.1038/sdata.2018.110
- 495 Ren X, Zhang H, Luo H. 2022. Dynamic emergence of relational structure network in human brains. *Progress in*
496 *Neurobiology* **219**:102373. doi:10.1016/j.pneurobio.2022.102373
- 497 Saffran JR, Aslin RN, Newport EL. 1996. Statistical Learning by 8-Month-Old Infants. *Science* **274**:1926–1928.
- 498 Schapiro AC, Rogers TT, Cordova NI, Turk- NB, Botvinick MM. 2013. Neural representations of events arise from
499 temporal community structure **16**:486–492. doi:10.1038/nn.3331.Neural
- 500 Schapiro AC, Turk-Browne NB, Botvinick MM, Norman KA. 2017. Complementary learning systems within the
501 hippocampus: A neural network modelling approach to reconciling episodic memory with statistical learning.
502 *Philosophical Transactions of the Royal Society B: Biological Sciences* **372**. doi:10.1098/rstb.2016.0049
- 503 Schapiro AC, Turk-Browne NB, Norman KA, Botvinick MM. 2016. Statistical learning of temporal community structure
504 in the hippocampus. *Hippocampus* **26**:3–8. doi:10.1002/hipo.22523
- 505 Stiso J, Lynn CW, Kahn AE, Rangarajan V, Szymula KP, Archer R, Revell A, Stein JM, Litt B, Davis KA, Lucas TH, Bassett
506 DS. 2022. Neurophysiological Evidence for Cognitive Map Formation during Sequence Learning. *eNeuro*
507 **9**:ENEURO.0361-21.2022. doi:10.1523/ENEURO.0361-21.2022
- 508 Todorovic A, de Lange FP. 2012. Repetition Suppression and Expectation Suppression Are Dissociable in Time in Early
509 Auditory Evoked Fields. *Journal of Neuroscience* **32**:13389–13395. doi:10.1523/JNEUROSCI.2227-12.2012
- 510 Toro JM, Trobalón JB. 2005. Statistical computations over a speech stream in a rodent. *Perception and Psychophysics*
511 **67**:867–875. doi:10.3758/BF03193539

513
514
515
516
517
518
519
520
521
522
523
524
525
526
527
528
529
530
531
532
533
534
535
536
537
538
539
540
541
542
543
544
545
546
547
548

Figure captions

Movie 1: Design and procedure. A) Example of a sparse community network for one participant. All community networks are similar in terms of properties, but New Within and New Between transitions are randomly drawn for each participant. Purple lines correspond to Familiar Within-community transitions, red lines to Familiar Between community transitions, and blue and pink lines correspond respectively to New Within and New Between transitions. We can derive a sequence by performing a random walk into this network (click to see video of the design). Here we display an example of a test sequence derived from this structure. B) Experimental procedure. First, participants passively listened to a sequence from a sparse community network, in which each TP between tones was 25% (Training). Then they were presented with six 960-items test blocks obtained from the community structure graph comprising New Within and Between community transitions with low transition probabilities of 4% (light blue and pink colors on the graph). C) Table summarizing the local and community properties for the transitions for each condition. Each single Familiar transition is, on average, presented 18.4 times/block (20 in the Training sequence) and, therefore, has a probability of 23% to be observed (25% in the training sequence) irrespectively of staying within or switching between communities. New transitions have a probability of 4% in the test blocks, which implies that each single New Transition is heard 3.2 times/block on average.

Figure 1 : *Within vs. Between community decoders on the MEG signal. Top Panel: Decoders with all Within community epochs (Familiar & New) vs. all Between communities epochs (Familiar & New) transitions. A) Generalization Across Time (GAT) matrix with significant cluster delineated in black. B) Time-by-time decoding. The shaded area indicates a significant temporal cluster. C. Individual performances based on whole epoch decoding: Mean Decoding accuracy across subjects (green bar, one dot per subject, the black line represents standard error). Those three analyses have been replicated with Familiar only transitions (middle panel) and New only transitions (bottom panel). Community structure was encoded in each case despite the flat local transition probability. Stars represent significance of the statistical tests (* $p < 0.05$, ** $p < 0.01$, *** $p < 0.001$).*

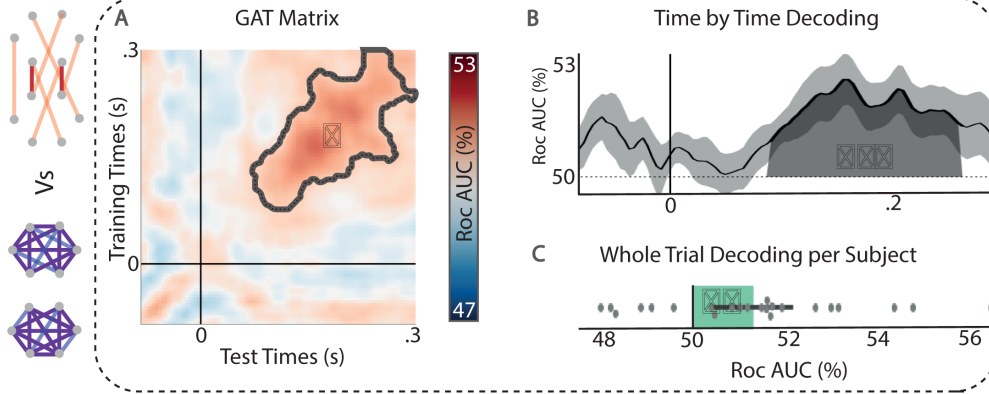
Figure 2 : Control analyses for the results presented in figure 2. For each decoder, we controlled for the current tone, the previous tone and the pair (both current and previous tone simultaneously). We also controlled for habituation due to temporal proximity between tones. All the analyses qualitatively and quantitatively confirmed previous results except the New Within vs. New Between control analysis that did not reach significance, probably because of the small number of epochs.

549

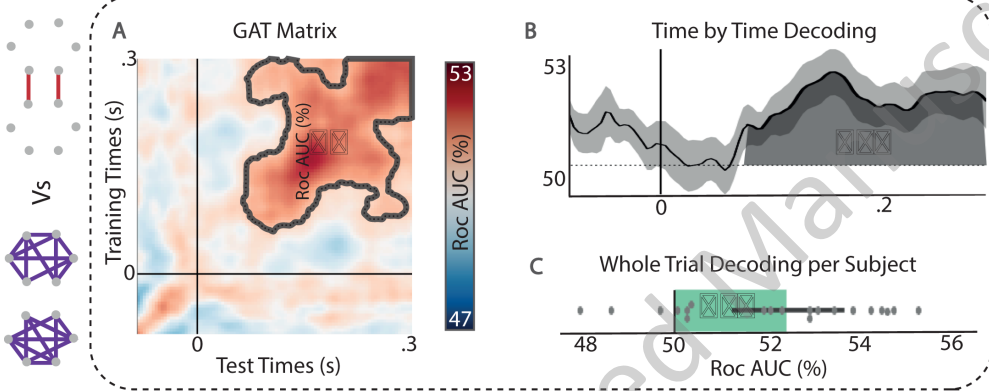
550 **Figure 3:** Associative learning estimation and fit on MEG data. A) Top: Decoding performance of the first item of the sequence across time (2.5s
551 window). Shaded colors indicate the Stimulus Onset Asynchrony (SOA) between each tone of the sequence. The dotted line shows the chance
552 level. Bottom: Decoding performance averaged over the duration of each tone and the following Inter Stimulus Interval (ISI). Error bars present
553 the standard error across subjects. It takes ~8 items for the decoder of the first tone to converge to chance level. B) Matrix of exact transition
554 probabilities (A) associated with the graph underlying the sequence. Familiar transitions are associated with 23% transition probabilities and New
555 with 4% (movie 1). Impossible transitions have a null transition probability. C) Estimation of the long-horizon associative learning strength for
556 each transition. Based on the decoder (panel A), we estimated the overlap between non adjacent elements of the sequence (average decoder
557 accuracy during SOA of item $n+i$). We then computed the associative learning strength (\hat{A} matrix) for each pair of elements as the sum of the
558 different transitional probability orders (A^i), weighted by the overlap between item representations. D) Average of the long-horizon associative
559 learning strength per condition. Pruning (Familiar Within > Familiar Between) and completion (New Within > New Between) effects are consistent
560 with behavioral results (Benjamin et al., 2023a) and with the decoding performance obtained in fig 1. E) Regression coefficient for the estimated
561 long horizon associative novelty
562 ($-\log(\hat{A})$) for each MEG sensor. Significant time-windows are shown in shaded areas and significant sensors are indicated on the t-map
563 topographies by the white dots. These were obtained with a spatio-temporal cluster-based permutation analysis. The red line below the sensors
564 value represents the time course of the average regression value on the sensors of the significant cluster.

565

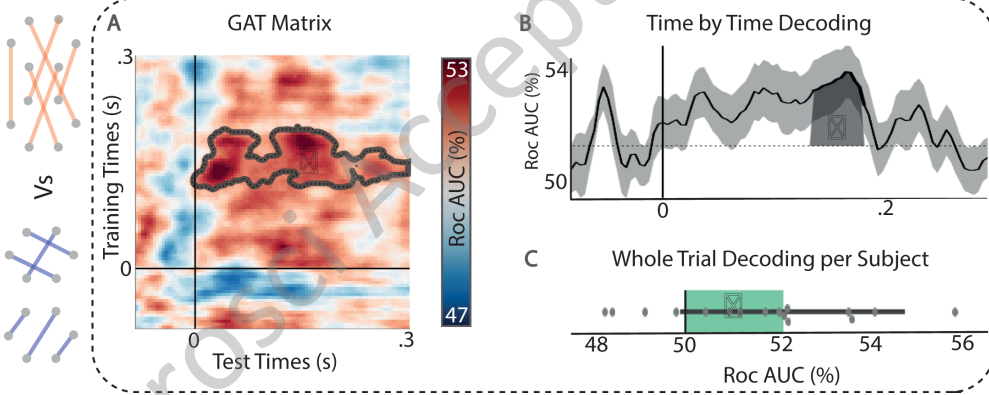
Within Vs Between

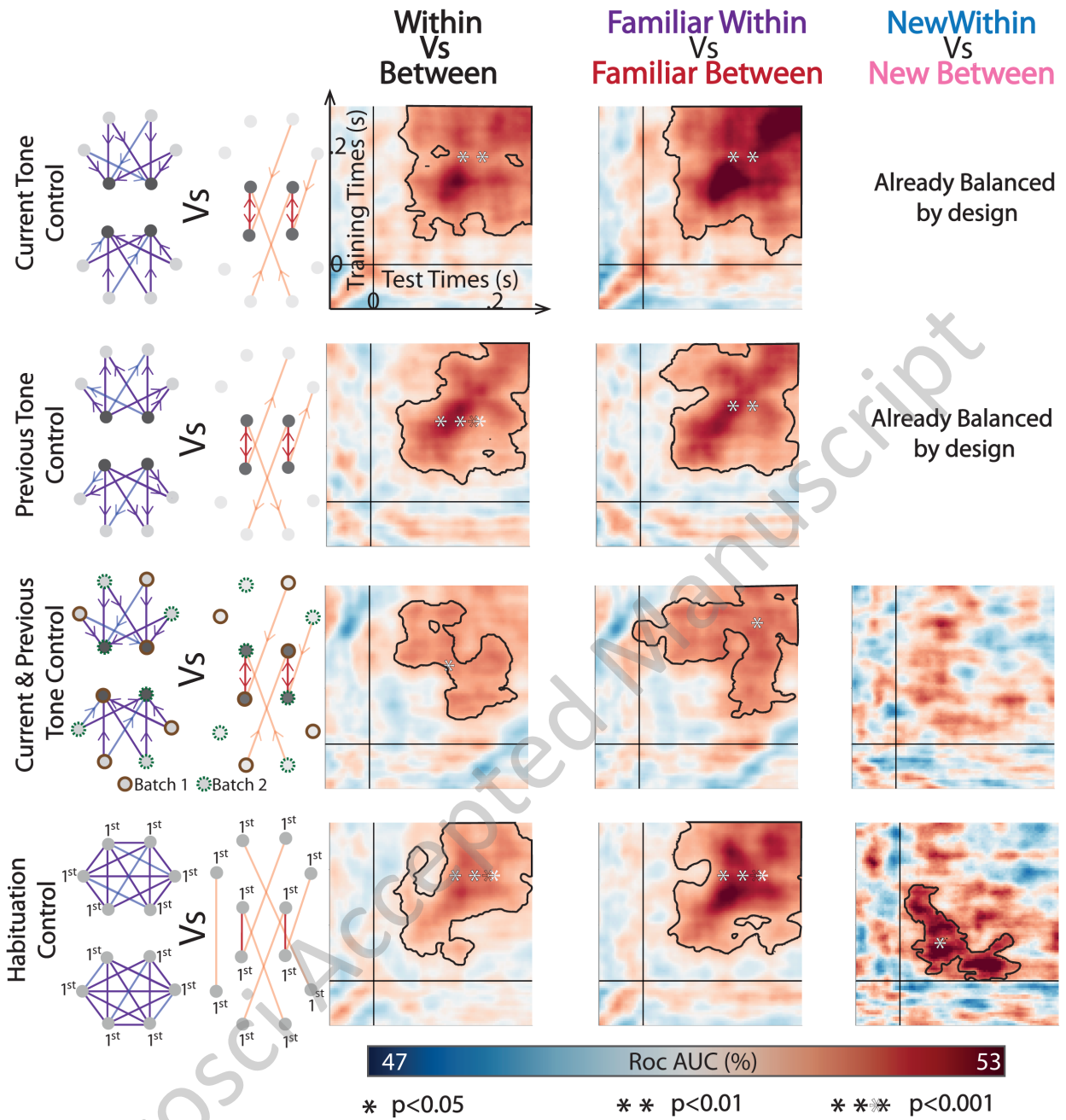


Familiar Within Vs Familiar Between

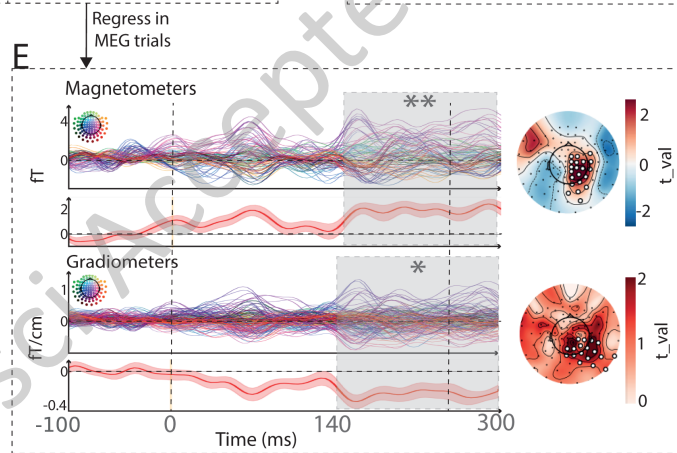
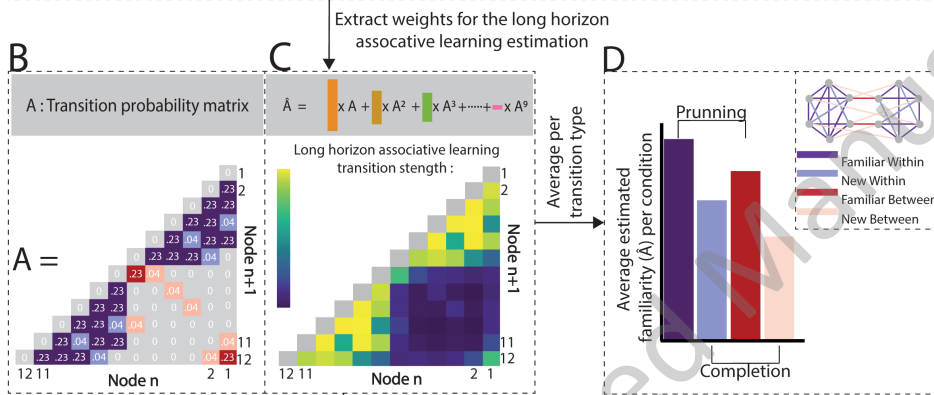
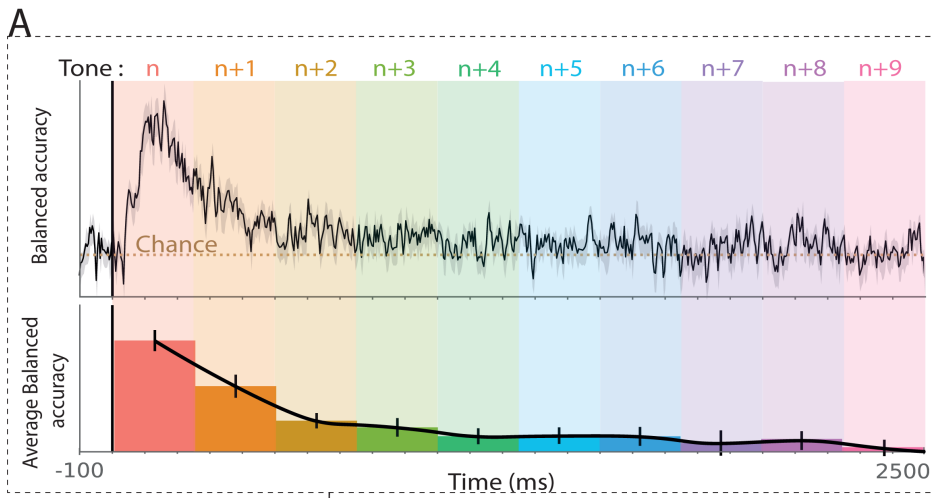


New Within Vs New Between

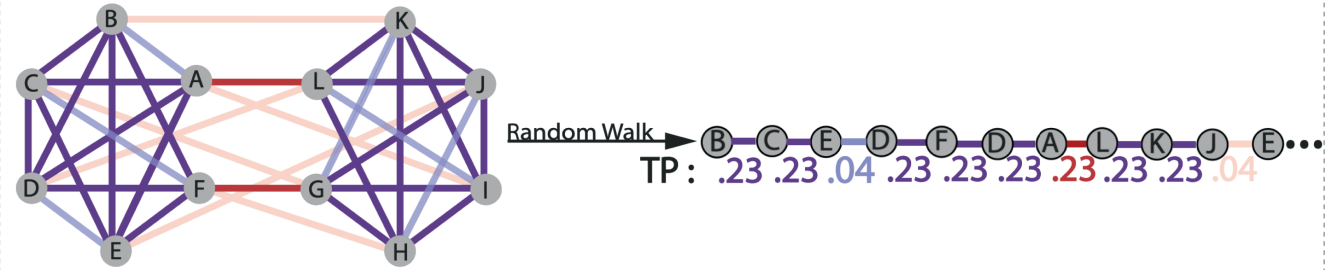




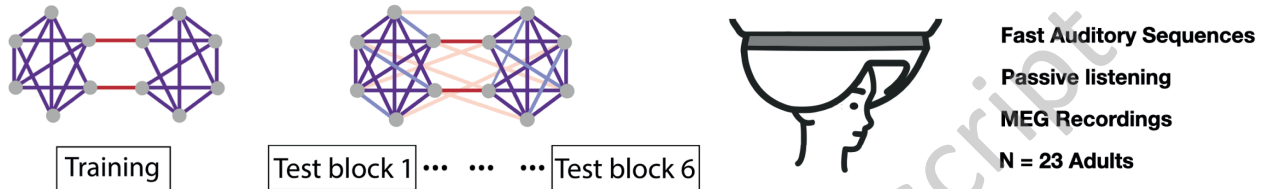
JNeurosci Accepted Manuscript



A : From Sparse Community Network to sequence



B : Procedure : Passive listening & MEG Recordings



C : Transitions properties

	Training		Test 1-6		Community
	TP	Freq	TP	Freq	
Familiar Within Community	0.25	20	0.23	18.4/block	Within
New Within Community	0	0	0.04	3.2/block	Within
Familiar Between Community	0.25	20	0.23	18.4/block	Between
New Between Community	0	0	0.04	3.2/block	Between

JNeurosci Accepted Manuscript